Localized processing by amacrine cells in the fly lamina: a cable model

Jansonius, NM; Jansen, M; Jongebloed, H; van Hateren, JH

Published in:
Information processing by spiking neurons in the first optic chasm of the blowfly : thesis

Publication date:
1998

Localized processing by amacrine cells in the fly lamina: a cable model

N.M. Jansonius*, M. Jansen, H. Jongebloed, J.H. van Hateren

Department of Biophysics, University of Groningen, Nijenborgh 4,
NL-9747 AG Groningen, The Netherlands

(November 18, 1997)

Abstract. The on-off and sustaining units in the first optic chiasm of the blowfly visual system are presumably third-order neurons, postsynaptic to the amacrine cells in the lamina. We modelled the cable properties of amacrine cells, and find that these are consistent with two characteristics of the on-off and sustaining units. The first characteristic is their poor temporal resolution compared to that of the photoreceptors, the second is their spatially localised processing, despite the fact that the anatomy of the amacrine cell suggests a wide receptive field.

1 Introduction

Photoreceptor cells in the fly visual system feed signals into two classes of postsynaptic cells, the Large Monopolar Cells (LMCs) and the amacrine cells (e.g., Shaw 1984). Each LMC connects one point in space with the central visual system (e.g., Laughlin 1980; van Hateren 1992). In contrast to that, the amacrine cell consists of an irregular array of slender dendrites, connecting photoreceptor input from many different viewing directions. The amacrine cell thus resembles horizontal and amacrine cells in the vertebrate retina.

In addition to the LMCs and amacrines, two spiking neurons have been described in the peripheral visual system of the fly (Arnett 1971, 1972; Jansonius and van Hateren 1991, 1993ab). One of them, the sustaining unit, responds with a sustained increase in spike rate to illumination. The other neuron, the on-off unit, responds with a transient increase in spike activity to both the onset and the cessation of illumination. The spatiotemporal properties of the spiking units differ in several respects from those of the photoreceptor. Compared with the photoreceptor, the sustaining unit has a slightly wider receptive field, and a substantially slower response. The receptive field of the on-off unit appears to consist of more or less independent subunits of which the response is summated. The spatial and temporal resolution of these subunits are again, as in the sustaining unit, lower than in the photoreceptor.

As discussed previously (Laughlin 1980, 1984; Shaw 1981, 1984; Jansonius and van Hateren 1993b), the spiking units presumably are the third-order neurons L4 and L5, post-synaptic to the amacrine cell (see Fig. 1). Interestingly, the receptive fields of the sustaining unit and the subunit of the on-off unit are much smaller than expected from the anatomy of the amacrine cell. This suggests that the amacrine cell in the fly might perform local processing (see also Shaw 1981, 1984) comparable to that described in the vertebrate retina (for horizontal cells see e.g. Lankheet et al. 1996). Unfortunately, in the fly, both the amacrine and the spiking units are too small for reliable intracellular recording and staining (see below). Therefore we modelled the cable properties of the amacrine cell in order to investigate whether passive signal conduction by the amacrine might be responsible for the two main properties of the on-off and the sustaining unit: (1) the local processing despite the fact that the anatomy of

* *Present address:* Dept. of Ophthalmology, University Hospital, Groningen
Correspondence to: J.H. van Hateren (Fax: +31 50 3634740; e-mail: hateren@bcn.rug.nl)

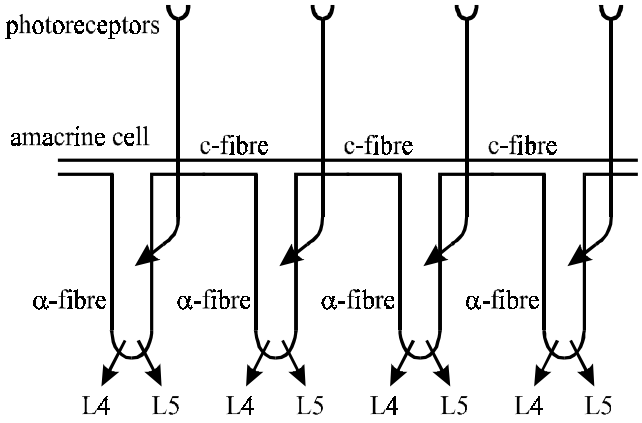

Fig. 1. Scheme of anatomical connections from photoreceptors to L4 and L5. Amacrine cells are directly postsynaptic to photoreceptor terminals; α-fibres (diameter approximately 0.4 μm) are connected by much thinner (approximately 0.05 μm) c-fibres. The α-fibres have output synapses to monopolar cells L4 and L5

the amacrine suggests a wide receptive field and (2) the lower temporal resolution of the on-off and the sustaining unit in comparison with the photoreceptor.

2 Methods and Results

2.1 Identification of the recording site of on-off and sustaining units

The validity of the model we develop here, where we use the anatomy of the amacrine cell for explaining the spatial and temporal properties of the sustaining and on-off unit, depends on the assumption that both units indeed connect lamina and medulla. Recent intracellular recordings from fly lamina and chiasm (Douglas and Strausfeld 1995) failed to find spiking cells. Although the extracellular recording site for measuring on-off and sustaining cells strongly suggests that the recordings are from the chiasm between lamina and medulla, and not, e.g., from distal parts of the medulla, we decided to stain the recording position in order to clarify this point. To this end we electrolytically plated a tungsten microelectrode with copper. After recording from an on-off or sustaining unit, copper was electrolytically deposited at the

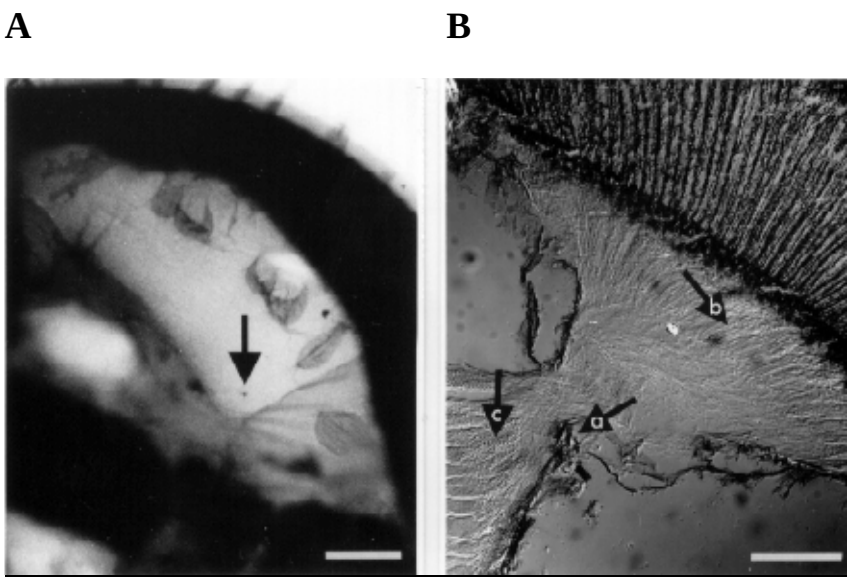

Fig. 2. Identification of the recording site for an on-off units. **A** Wholemount view showing the stained spot (arrow) at the recording site. The photograph shows a rear view of the right eye with partly opened head capsule (up=dorsal). Scale bar: 230 μm. **B** Horizontal section of the same eye as in A (up=frontal), showing the staining and lesion at the recording site in the chiasm (arrow a). Arrows b and c point to the lamina neuropile and layer of medulla cell bodies, respectively. Scale bar: 100 μm. See text for further details.

recording site. The electrode was then carefully removed, and the head capsule of the fly was further opened. The visual lobes were subsequently fixated, and the copper deposited was stained with rubeanic acid (Uzman 1956). In wholemount, the recording position was then visible as a small dark spot (Fig. 2A). We successfully performed this experiment in 8 flies, and always found a position both consistent with the position of the electrode observed during the recording, and consistent with a recording site in the chiasm. In three of these flies, the brain was dehydrated, embedded in paraphine, and sliced (in sections of 30 μm) parallel to the original direction of the electrode. Figure 2B shows for one fly the section with the densest staining at the recording site (arrow a; the staining surrounds a small lesion caused by removing the electrode after several hours of recording). Sections above and below this one were less strongly stained, or not at all. Similar results were obtained in the other two sectioned flies. The position of the recording site is in the chiasm, remote from both the lamina (arrow b) and the layer with cell bodies in the medulla (arrow c). Thus we conclude that the recording is from spiking neurons running through the chiasm, and not from neurons in the distal part of the medulla.

That these cells were not encountered by intracellular recording (Douglass and Strausfeld 1995) is probably due to their very small size. If they are identical to the anatomically identified L4 and L5, the axons have diameters of approximately 0.8 μm (Strausfeld 1971). These diameters are not sufficiently larger than the tip diameters of present-day glass micropipettes to allow reliable intracellular recording. Moreover, even if an impalement would succeed, the leakage resistance induced by the impalement would be very much larger than the input impedance of the cell. As a result, the cell would be very far from its normal (electro)physiological operating mode.

2.2 Towards a cable model

The temporal frequency response of the photoreceptor, the sustaining unit, and the on-off unit are shown at a single intensity in Fig. 3, all for a wide-field stimulus. Both the curves for the sustaining and the on-off unit are low-pass filtered as compared with the corresponding curve for the photoreceptor. The curves of the sustaining and on-off cell reach 50% of their

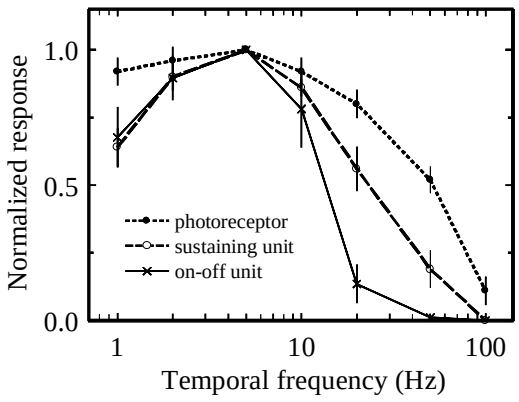

Fig. 3. Normalized temporal frequency response of the photoreceptor, the sustaining unit, and the on-off unit. The wide-field stimulus was sinusoidally modulated in time. Responses of photoreceptors and sustaining units were taken as the amplitude of the resulting response modulation, responses of on-off units as the average spike rate. Data from Jansonius and van Hateren (1991, 1993b)

maximum response at 25 Hz and 14 Hz, respectively, compared with 50 Hz for the photoreceptor. We hypothesize here that the major part of this low-pass filtering is caused by the passive cable properties of the amacrine cell, and below we will require that this low-pass filter reaches 50% of its maximum response at an average value of 20 Hz. The difference between on-off and sustaining cells must then have a more proximal origin.

The sustaining unit and the subunit of the on-off unit have small receptive fields (2° and 2.3°, respectively, Jansonius and van Hateren 1993a,b), only slightly broader than that of the

photoreceptor (1.4°, Smakman et al. 1984; van Hateren 1984). Therefore, the amacrine cell, although anatomically very wide (connecting up to 17 cartridges, see Shaw 1981, after Strausfeld 1976), apparently does not average the photoreceptor inputs over a large area. We approximate the receptive fields of the photoreceptors as Gaussians with a half-width of 1.4° and an effective one-dimensional separation of 1.5° (e.g., van Hateren 1990). Then we find that, for a one-dimensional array of photoreceptors, a 30-50% signal transfer to neighbouring cartridges produces the required receptive fields of 2-2.3°. Below we can now investigate whether the passive cable properties of the amacrine cell can produce not only this limited signal transfer from one cartridge to the next, but also the right amount of low-pass filtering.

We find that it is not possible to produce the required temporal and spatial properties at the same time by simply modelling the amacrine cell as a single passive cable, connecting the cartridges laterally (Fig. 4A). From published anatomical micrographs (Shaw 1981, 1984; Meinertzhagen and O'Neil 1991) we estimate that the dendrites of the amacrines have diameters ranging between 0.05 and 0.5 μm. Within this diameter range, we find that local processing (30-50% signal transfer to the next cartridge) is only possible with low membrane resistances. These low membrane resistances, however, make the cable at least an order of magnitude too fast for explaining the observed temporal low-pass filtering.

An anatomically more realistic model is shown in Fig. 4B. Here, the α-processes of the amacrine cell (diameter 0.3-0.5 μm) are connected by much thinner fibres (diameter 0.05-0.1 μm). Below we will refer to these as α-fibres and c-fibres, respectively. As shown in Fig. 4B, we model each α-fibre and each c-fibre as a cable segment. The cable model is based on the theory described in van Hateren (1986; see e.g. van Hateren and Laughlin, 1990, for an application to LMCs). Each cable segment is replaced by a T-circuit, consisting of three components of which the impedances are determined by the parameters of the segment: length, diameter, membrane resistance, membrane capacitance (here taken as 1 $\mu F/cm^2$), and axial resistance (here taken as 0.08 kΩ·cm). The circuit of Fig. 4B was evaluated in the frequency domain using first a ladder algorithm (see van Hateren 1986) on each half of the circuit (as

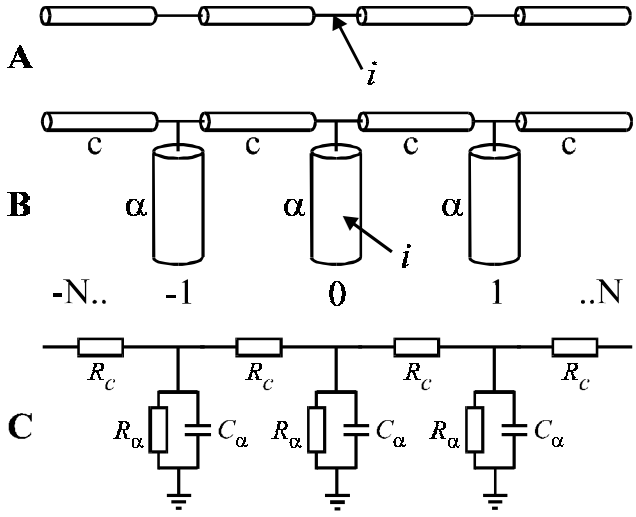

Fig. 4. A Simple cable model of the amacrine cell, with short cable segments connecting neighbouring cartridges. This model can not produce the required spatial and temporal properties. **B** More realistic cable model of the amacrine cell: c-fibres connect the α-fibres entering neighbouring cartridges. Both α-fibres and c-fibres are modelled as short cable segments. The model enables calculating the effect of injecting a current *i* (caused by the photoreceptor-amacrine synapse) into an α-fibre, both the effect on the α-fibre itself and on its neighbours. **C** Approximate equivalent to the scheme of **B** (see text for explanation)

seen from the site of current injection, i.e. α-fibres 1,2,...,*N* and -1,-2,...,-*N*, respectively). This yielded the input resistance of each half, and thus the total input resistance as seen by α-fibre 0. Injecting a short current pulse in α-fibre 0 then yields the voltage in α-fibre 0 and subsequently in each of the other α-fibres. With the parameter values used in the model, each α-fibre is approximately isopotential. The c-fibres have such a small diameter that their axial resistance (R_c) dominates their properties. As a result, the scheme of Fig. 4B is roughly equivalent to the scheme of Fig. 4C. In the latter scheme it is easy to see how the model functions. Its temporal low-pass properties are mainly caused by the RC-time of the α-fibre membrane ($\tau=R_\alpha C_\alpha$). Local processing is caused by the fact that each R_α-R_c-node acts as a voltage divider, reducing the voltage transferred from one α-fibre to the next. Local processing then results if R_c is at least of the same order of magnitude as R_α.

Many of the parameters needed for the model can be inferred from published anatomical measurements. EM photographs provide estimates for the diameter of the α-fibre: 0.3-0.5 μm (Shaw 1981, 1984; Meinertzhagen and O'Neil 1991). The α-fibre extends over the whole depth of the cartridge (approximately 50 μm in *Calliphora*, Strausfeld 1971) and presumably runs back in the same cartridge (Shaw 1981, Strausfeld and Nässel 1980; yielding a length of no more than 100 μm). The diameter of the c-fibres is clearly much smaller than that of the α-fibres. The smallest fibres of any type in the EM photographs of *Drosophila* by Meinertzhagen and O'Neil (1991) appear to be approximately 50 nm in diameter, yielding 35 nm as a lower limit for the inner diameter (estimating the thickness of the cell membrane as maximally 7.5 nm). *Drosophila* is the smallest species examined, so that these dimensions appears to be the minimum expected in any fly. The length of each c-fibre segment equals at least the distance between two adjacent cartridges, i.e., approximately 10 μm (Strausfeld 1971). Each segment might be considerably longer, however, because it possibly connects the proximal side of one α-fibre with the distal end of another (Strausfeld and Nässel 1980). In *Musca*, there are about 500 amacrines in 2800 cartridges, and each cartridge is visited by 3 amacrines (Strausfeld and Campos-Ortega 1977). Thus each amacrine then extends into 17 cartridges (cf. 6-17, Shaw 1981), i.e. N=8 in the model.

Table 1 shows that the model of Fig. 4B produces results that are consistent with the measurements from the sustaining and the on-off unit. The required A_r of 30-50% (relative signal transfer to neighbouring cartridge) and f_c of 20 Hz (cut-off frequency at 50% of maximum response) are possible for realistic values of the parameters, and are not very sensitive to variations of these parameters within their expected range. The parameters used are the diameter, length, and membrane resistance of the α- and c-fibres, and the total number of α-fibres. Anatomical measurements as discussed above give estimates for diameters and lengths, and for the number of α-fibres. The membrane resistance of the c-fibre does not influence the model calculations as long as it is larger than 4 $k\Omega \cdot cm^2$ (cf. the 100 $k\Omega \cdot cm^2$ estimated by van Hateren and Laughlin 1990 for the membrane of the LMC axon, a membrane with presumably extremely few ion channels). Thus the only important unknown parameter is the membrane resistance of the α-fibre. We find that values in the range of 20-45 $k\Omega \cdot cm^2$ resulted in both the right amount of temporal low-pass filtering and the right amount of local processing.

2.3 Extending the model to two dimensions

Above, we have approximated the anatomy of the amacrine cell as a one-dimensional model, with all c- and α-fibres aligned in a single, regular row. In reality, the amacrine cell is spread out in two dimensions, connecting a patch in the visual image, and not just a line. Furthermore, the pattern of connections appears to be quite irregular (see Shaw 1991), with connections only well-defined in a statistical sense. In order to assess the influence of these two factors, we made a two-dimensional model of the amacrine cell using the software package Genesis (Bower and

Table 1 Spatial and temporal behaviour of a cable model of the amacrine cell

parameter (dimension)	default value	alternative values	A_r (-)	f_c (Hz)
			default 0.37	default 20
l_α (μm)	100	50	0.49	21
d_α (μm)	0.4	0.3	0.40	21
		0.5	0.33	19
R_α (kΩ.cm^2)	27	20	0.30	25
		45	0.45	14
l_c (μm)	50	10	0.56	27
		100	0.26	17
d_c (μm)	0.05	0.035	0.26	18
		0.1	0.54	25
R_c (kΩ.cm^2)	100	4	0.30	25
		200	0.37	20
N (-)	8	4	0.37	20
		16	0.37	20

Table 1. A_r: relative signal transfer to neighbouring cartridge; f_c: cut-off frequency (at 50% of maximum response); l_α: length of α-fibre; d_α: diameter of α-fibre; R_α: membrane resistance of α-fibre; l_c: length of c-fibre; d_c: diameter of c-fibre; R_c: membrane resistance of c-fibre; N: number of cable nodes in one direction. The default parameters in the second column lead to the default A_r and f_c shown in the second row, the other values of A_r and f_c result from changing a single parameter to an alternative value in the third column, whilst keeping all other parameters fixed to their default value

Beeman 1994), and we varied the regularity of the geometry. We found that the two-dimensional model produces a relative signal transfer to neighbouring cartridges (A_r) and a temporal cut-off frequency (f_c) in the same range as those calculated for the one-dimensional model, and that A_r and f_c are quite robust against variations in the precise geometry of the neuron. This is caused by the fact that signals from an α-fibre mainly spread to direct neighbours, whereas α-fibres further away are relatively little affected.

3 Discussion

In this article we showed, firstly, that the anatomy of the amacrine cell is well suited to produce, through passive cable properties, two properties found in the on-off and sustaining cells. The first property is the lower temporal acuity of these cells compared with the photoreceptor, the second the localised processing required from the amacrine cell despite its anatomical wideness. Localised processing is consistent with the fact that the spatial resolving power (i.e., the highest spatial frequency responded to) of the on-off and sustaining cells is only slightly smaller than that of the photoreceptor. Thus, the model of Fig. 3B, though only a coarse approximation of the rather complex anatomy of the amacrine cell, appears to capture the essential characteristics of the cell. As shown in Table 1, various realistic combinations of parameters yield similar results.

The membrane resistance we infer for the α-fibre is rather high. It gives a total conductance for one α-fibre of 50 pS. The conductance of single ion channels lies typically in the range of 5-50 pS (Hille 1984). The number of synapses onto each α-fibre is not known, but it may be considerable because the α-fibre is a post-synaptic element in part of the lamina tetrads (see, e.g., Shaw 1984). This means that the synaptic channels in the α-fibre must have a low conductance each and/or must be in the open state for only a small percentage of the time. The low conductance of the α-fibre is not unreasonable from the point of view of homeostasis. The amacrine cell dendrite has a very unfavourable surface-volume ratio, and thus relatively little

space is left for mitochondria which have to deliver the metabolic energy for maintaining ionic balance.

Shaw (1984) reported a hyperpolarizing response, recorded in the lamina of *Calliphora*, that could only be elicited by stimulating one single facet. His interpretation that this recording may have come from a disconnected α-process is consistent with our present model: the resistances inferred here lead to α-fibres that are to a large extent independent from each other, and that thus may be driven by a single photoreceptor.

In a single experiment we stimulated a recorded sustaining cell both at on-axis and at various off-axis positions. We found that the latency became progressively larger for more off-axis stimulation: the time to peak increased off axis up to about 80 ms, compared with 30 ms for on-axis stimulation. In fact, this is consistent with the delays we expect from passive propagation of the signal through the amacrine cell. The observed latency would not be consistent, however, with an alternative hypothesis that the low-pass filtering is entirely caused by, e.g., the slowness of one of the synapses in the neural chain from photoreceptor to sustaining unit. This reinforces our interpretation that at least part of the low-pass filtering is caused by the membrane time constant of the α-fibre.

Finally, we should stress that the temporal characteristics of the on-off and sustaining cells are not identical (Fig. 3). Thus if our model is correct, the remaining differences must have their origin later than the amacrine cell, e.g., arising from slightly different properties of the synapses from amacrine cells to the on-off and sustaining cells, respectively.

Acknowledgements. We thank Ian Meinertzhagen, Kees Schilstra, and Doekele Stavenga for comments, and we thank especially Ian Meinertzhagen for advising us on the anatomy of amacrine cells. This research was supported by the Netherlands Organization for Scientific Research (NWO).

References

Arnett DW (1971) Receptive field organization of units in the first optic ganglion of diptera. Science 173:929-931

Arnett DW (1972) Spatial and temporal integration properties of units in first optic ganglion of dipterans. J Neurophysiol 35:429-444

Bower JM, Beeman D (1994) The book of GENESIS: exploring realistic neural models with the GEneral NEural SImulation System'. Springer, New York

Douglass JK, Strausfeld NJ (1995) Visual motion detection circuits in flies: peripheral motion computation by identified small-field retinotopic neurons. J Neuroscience 15:5596-5611

Hateren JH van (1984) Waveguide theory applied to optically measured angular sensitivities of fly photoreceptors. J Comp Physiol A 154:761-771

Hateren JH van (1986) An efficient algorithm for cable theory, applied to blowfly photoreceptor cells and LMCs. Biol Cybernetics 54:301-311

Hateren JH van (1990) Directional tuning curves, elementary movement detectors, and the estimation of the direction of visual movement. Vision Res 30:603-614

Hateren JH van (1992) Theoretical predictions of spatiotemporal receptive fields of fly LMCs, and experimental validation. J.Comp.Physiol. A 171:157-170

Hateren JH van, Laughlin SB (1990) Membrane parameters, signal transmission, and the design of a graded potential neuron. J Comp Physiol A 166:437-448

Hille B (1984) Ion channels of excitable membranes. Sinauer Associates, Sunderland Mass.

Jansonius NM, Hateren JH van (1991) Fast temporal adaptation of on-off units in the first optic chiasm of the blowfly. J Comp Physiol A 168:631-637

Jansonius NM, Hateren JH van (1993a) On-off units in the first optic chiasm of the blowfly. II: Spatial properties. J Comp Physiol A 172:467-471

Jansonius NM, Hateren JH van (1993b) On spiking units in the first optic chiasm of the blowfly. III. The sustaining unit. J Comp Physiol A 173:187-192

Lankheet MJM, Rowe MH, Wezel RJA van, Grind WA van de (1996) Spatial and temporal properties of cat horizontal cells after prolonged dark adaptation. Vision Res 36:3955-3968

Laughlin SB (1980) Neural principles in the visual system. In: Autrum H (ed) Handbook of Sensory Physiology, vol VII/6B. Springer, Berlin Heidelberg New York, pp 133-280

Laughlin SB (1984) The roles of parallel channels in early visual processing by the arthropod compound eye. In Ali MA (ed) Photoreception and vision in invertebrates. Plenum, New York London, pp 457-481

Meinertzhagen IA, O'Neil SD (1991) Synaptic organization of columnar elements in the lamina of the wild type in *Drosophila melanogaster*. J Comp Neurol 305:232-263

Shaw SR (1981) Anatomy and physiology of identified non-spiking cells in the photoreceptor-lamina complex of the compound eye of insects, especially Diptera. In Roberts A, Bush BMH (eds) Neurons without impulses. Cambridge University Press, Cambridge, pp 61-116

Shaw SR (1984) Early visual processing in insects. J Exp Biol 112:225-251

Smakman JGJ, Hateren JH van, Stavenga DG (1984) Angular sensitivity of blowfly photoreceptors: intracellular measurements and wave-optical predictions. J Comp Physiol A 155:239-247

Strausfeld NJ (1971) The organization of the insect visual system (light microscopy). I. Projections and arrangements of neurons in the lamina ganglionaris of diptera. Z Zellforsch 121:377-441

Strausfeld NJ (1976) Mosaic organizations, layers, and visual pathways in the insect brain. In Zettler F, Weiler R (eds) Neural principles in vision. Springer, Berlin Heidelberg New York, pp 245-279

Strausfeld NJ, Campos-Ortega JA (1977) Vision in insects: pathways possibly underlying neural adaptation and lateral inhibition. Science 195:894-897

Strausfeld NJ, Nässel DR (1980) Neuroarchitectures serving compound eyes of crustacea and insects. In: Autrum H (ed) Handbook of Sensory Physiology, vol VII/6B. Springer, Berlin Heidelberg New York, pp 1-132

Uzman LL (1956) Histochemical localization of copper with rubeanic acid. Laboratory Investigation 5:299-305